

# Dielectric responses of the layered cobalt oxysulfide $\text{Sr}_2\text{Cu}_2\text{CoO}_2\text{S}_2$ with $\text{CoO}_2$ square-planes

S. Okada\* and I. Terasaki

*Department of Applied Physics Waseda University, Tokyo 169-8555, Japan and  
CREST, Japan Science and Technology Agency, Tokyo 108-0075, Japan*

H. Ooyama and M. Matoba

*Department of Applied Physics and Physico-Informatics, Keio University, Yokohama 223-8522, Japan*

(Dated: November 20, 2018)

We have studied the dielectric responses of the layered cobalt oxysulfide  $\text{Sr}_2\text{Cu}_2\text{CoO}_2\text{S}_2$  with the  $\text{CoO}_2$  square-planes. With decreasing temperature below the Néel temperature, the resistivity increases like a semiconductor, and the thermopower decreases like a metal. The dielectric constant is highly dependent on temperature, and the dielectric relaxation is systematically changed with temperature, which is strongly correlated to the magnetic states. These behaviors suggest that carriers distributed homogeneously in the paramagnetic state at high temperatures are expelled from the antiferromagnetically ordered spin domain below the Néel temperature.

Many layered transition-metal oxides and sulfides have been the subject of the experimental and theoretical investigations, because they exhibit unusual physical properties originating from the strong electron correlation. From the viewpoint of materials design, we have studied the prototypical transition-metal hybrid material  $\text{Sr}_2\text{Cu}_2\text{CoO}_2\text{S}_2$  [1]. Layered cobalt oxysulfide  $\text{Sr}_2\text{Cu}_2\text{CoO}_2\text{S}_2$  crystallizes in an unusual intergrowth structure consisting of the  $\text{CoO}_2$  square lattice and  $\text{ThCr}_2\text{Si}_2$ -type sulfide layers, as shown Figure 1.

$\text{Sr}_2\text{Cu}_2\text{CoO}_2\text{S}_2$  exhibits rich and complicated magnetism, and shows successive transitions. First, it shows an antiferromagnetic transition with the Néel temperature  $T_N=190$  K which is detected by the neutron powder diffraction (NPD).  $M/H$  in Figure 2 (a) shows a broad maximum near 250 K, being indicative of 2D antiferromagnetic nature, as is normally seen for antiferromagnetic  $\text{K}_2\text{NiF}_4$ -type compounds. Below  $T_{N2}=125$  K, additional peaks appear in the NPD pattern, which suggests that interlayer magnetic correlation is grown. Below  $T_{SG}=80$  K,  $\text{Sr}_2\text{Cu}_2\text{CoO}_2\text{S}_2$  has a hysteresis behavior between field-cooled and zero-field-cooled magnetization curves, as is often seen in frustrated spin systems [2, 3, 4].

In transition-metal compounds, charge and spin degrees of freedom interact with each other to induce unconventional physics, such as high-temperature superconductivity in Cu oxides. Thus, in order to explore effects of magnetic excitations on charge transport of  $\text{Sr}_2\text{Cu}_2\text{CoO}_2\text{S}_2$ , we have measured electrical resistivity ( $\rho$ ), thermopower ( $S$ ) and dielectric constant ( $\epsilon$ ) of polycrystalline samples.

Polycrystalline samples of  $\text{Sr}_2\text{Cu}_2\text{CoO}_2\text{S}_2$  were prepared by a solid-state reaction[2, 3].

The resistivity was measured by a four-probe method, and the thermopower was measured using a steady-state technique from 4.2 from 300 K in a liquid He cryostat. The dielectric constant ( $\epsilon_1$ ) and ac conductivity ( $\sigma_{ac}$ ) were measured with a parallel plate capacitor arrange-

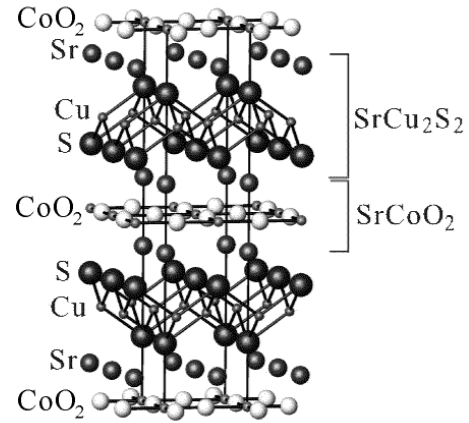


FIG. 1: Crystal structure of  $\text{Sr}_2\text{Cu}_2\text{CoO}_2\text{S}_2$  which crystallizes in an unusual intergrowth structure with the stacking sequence -Sr-Cu<sub>2</sub>S<sub>2</sub>-Sr-CoO<sub>2</sub>-Sr- (space group  $I/4mmm$ ) [3].

ment using an ac two-contact four-probe method with an LCR meter (Agilent 4284A) from  $10^2$  to  $10^6$  Hz. Owing to the two-probe configuration, the contact resistance and capacitance might have affected the measurement. However, the contact resistance was less than  $1 \Omega$ , which was much smaller than the sample resistance ( $50 \Omega$  at 200 K). In fact, the observed  $\sigma_{ac}$  was quantitatively consistent with the observed dc resistivity for  $\omega \rightarrow 0$ . Though we did not evaluate the contact capacitance, we can employ an evaluated value of 500 pF for  $\text{La}_2\text{CuO}_4$  from Ref. [5], because the contact capacitance is primarily determined by the area of the contact. It gives a reactance of  $3 \times 10^5 \Omega$  at 1 kHz, which is  $10^5$  times larger than the contact resistance. As a result, we can safely assume that our contact is primarily a resistive coupling, and can neglect the contact capacitance. We should further note that we tested different contact configurations of the same sample, and got identical results within experimental errors.

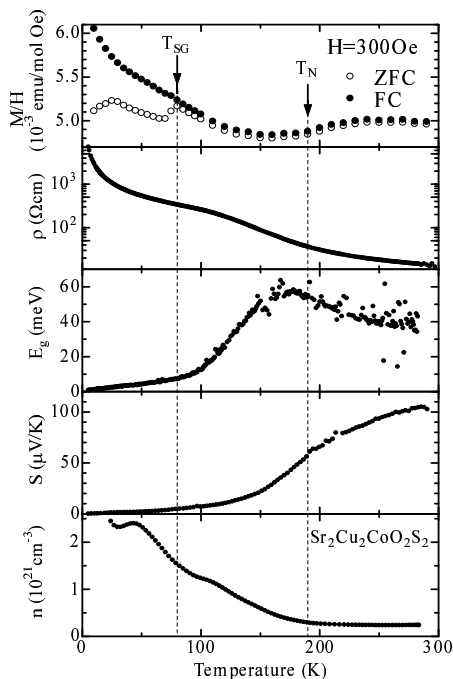


FIG. 2: Temperature dependences of (a) field-cooled and zero-field-cooled magnetic susceptibilities, (b) electrical resistivity ( $\rho$ ), (c) activation energy estimated from  $\rho$ , (d) thermopower ( $S$ ), and (e) local carrier density estimated from  $S$ .

Thus we conclude that the contact would not affect the measured  $\varepsilon$  within experimental errors of 1%.

Figure 2 (b) shows the temperature dependence of  $\rho$ . The  $\rho$  increases with decreasing temperature, which indicates that  $\text{Sr}_2\text{Cu}_2\text{CoO}_2\text{S}_2$  is a semiconductor. As is clearly shown, the temperature dependence of  $\rho$  is not a simple activation type. In particular,  $\rho$  shows a “plateau” near 50-120 K, indicating that this material is more metallic than a conventional semiconductor with a constant activation energy. In order to see this more clearly, the activation energy ( $E_g$ ) estimated from the relation as

$$\rho(T) = \rho_0 \exp(E_g/k_B T), \quad (1)$$

is plotted as a function of temperature in Fig. 2 (c). As expected,  $E_g$  depends on temperature. In particular,  $E_g$  suddenly decreases below around  $T_N$ , and is as small as  $E_g \sim k_B T$  below around  $T_{SG}$ . This suggests the carriers feel essentially no energy gap, and can move more freely at low temperature. In this sense, the electronic state below  $T_{SG}$  is “metallic” rather than semiconductive.

Figure 2 (d) shows the temperature dependence of  $S$ .  $S$  decreases with decreasing temperature, and  $S/T$  is as small as  $S/T$  of conventional metals below around  $T_{SG}$ . This seems to indicate that  $\text{Sr}_2\text{Cu}_2\text{CoO}_2\text{S}_2$  is a metal at low temperatures, and is consistent with the anomalously small  $E_g$ . In the lowest order approximation,  $S$  is

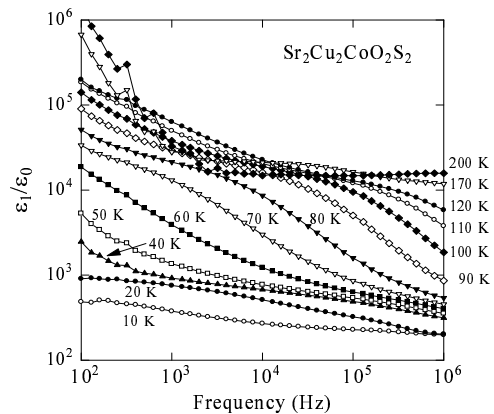


FIG. 3: Frequency dependence of dielectric constant.

expressed as functions of the carrier concentration ( $n$ ) as

$$|S| = \frac{\pi k_B^2}{2\hbar^2 d_c e} \frac{m}{n} T, \quad (2)$$

where  $d_c$  ( $=17.7 \text{ \AA}$ ) is the inter-layer spacing,  $e$  ( $> 0$ ) is the unit charge, and  $m$  is the bare electron mass [6]. Fig. 2 (e) shows the temperature dependence of  $n$ . Quite anomalously,  $n$  increases with decreasing temperature below  $T_N$ , which could not happen in a homogeneous system.

Suppose that the carriers (holes) and magnetic spins are segregated in the sample. Then the electric current flows in a filamentary path of the hole-rich region connected in a percolation network across the sample. In this situation,  $n$  observed from  $S$  should be the carrier density in the filamentary path. If the volume fraction of the filaments are 10 %,  $n$  would be 10 times larger than  $n$  distributed homogeneously. The large  $n$  and the small  $E_g$  naturally suggest that the carriers are segregated to form a percolation network below  $T_N$ .

Reflecting the successive phase transitions, the dielectric response is quite complicated. Figure 3 shows  $\varepsilon_1$  of  $\text{Sr}_2\text{Cu}_2\text{CoO}_2\text{S}_2$  as a function of frequency. Let us begin with the data at 10 K.  $\varepsilon_1$  shows a step-like decrease with increasing frequency, which is a dielectric relaxation. With increasing temperature, additional tails appear in  $\varepsilon_1$  at low frequencies above 40 K and 80 K, which means that another relaxation process begins to overlap. The tail extends to higher frequencies with increasing temperature, and low-frequency  $\varepsilon_1$  increases. Dielectric relaxation is more clearly seen in the so-called Cole-Cole plot for various temperatures (figure 4). in which the imaginary part of dielectric constant ( $\varepsilon_2$ ) is plotted as a function of  $\varepsilon_1$ . Here we calculated  $\varepsilon_2$  from  $\sigma$  as  $\varepsilon_2/\varepsilon_0 = (\sigma - \sigma_{dc})/\omega\varepsilon_0$ , where  $\sigma_{dc}$  is the dc conductivity. At 10 K, the data draws a single distorted semicircle, indicating the dielectric relaxation. With increasing temperature, additional relaxations begin to overlap, and the data draw two semicircles. Note that the three re-

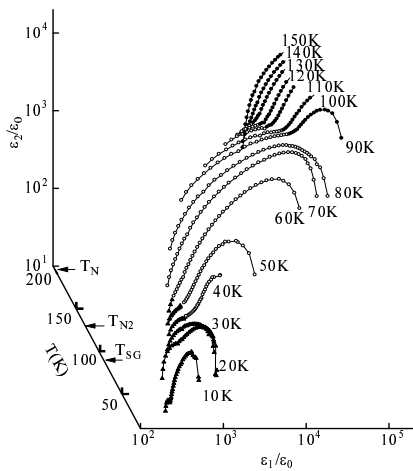


FIG. 4: Temperature dependence of the Cole-Cole plot. Three relaxations are plotted with different marks.

laxations are related to the magnetic transitions. The lowest-temperature relaxation corresponds to the hysteresis region from 10 to 50 K. The second relaxation corresponds to the second antiferromagnetic phase below 120 K ( $\sim T_{N2}$ ), and the highest-temperature relaxation corresponds to the first antiferromagnetic phase below  $T_N$ .

Let us discuss the origin of the dielectric relaxation. It should be emphasized that the observed relaxation is unique, and at least three relaxations appear with various magnetic phases. Since we used polycrystalline samples, we cannot exclude a possibility that this anomaly comes from grain boundaries. As Lunkenheimer *et al.* [7] have pointed out, anomalously large  $\epsilon_1$  at low frequencies might be related to a depletion layer at the grain boundaries, what is called “leaky capacitor” effect [8]. However,  $\epsilon_1$  in the low-frequency limit is almost independent of temperature in the leaky capacitor, whose temperature and frequency dependences are different from our data. Additionally, the coincidence between the dielectric relaxations and magnetic phase transitions is too orderly.

As mentioned above, we propose a self-organization or phase-separation of holes takes place in  $\text{Sr}_2\text{Cu}_2\text{CoO}_2\text{S}_2$ . According to this picture, the charge density is inhomogeneous in the sample, which could be vibrated by an external ac field to give large dielectric response. Below  $T_N$ , the holes are gradually confined in the percolation network and the spin-rich region (highly resistive) increases in volume. Thus the electronic network is near the percolation threshold near  $T_N$ , and goes far away from it with decreasing temperature. The dielectric constant of percolation systems consisting of metal and insulator nanocomposites has been extensively investigated. Recently Pakhomov *et al.* have reported that it diverges at low fre-

quencies near the percolation threshold [9], whose spectrum is very similar to the 200 K data in Fig. 3. At low temperatures, a sample away from the threshold in the insulating side shows a flat dielectric constant [10], which is also very similar to the data in Fig. 3. For more quantitative analysis, we need the same measurement with single crystal samples.

In summary, we have measured the resistivity, thermopower, dielectric constant and ac conductivity of polycrystalline samples of  $\text{Sr}_2\text{Cu}_2\text{CoO}_2\text{S}_2$ . All the transport parameters show characteristic change below  $T_N$ , which clearly indicates that the charge transport is highly correlated to the spin state. In particular, the qualitatively different dielectric relaxations are observed with decreasing temperature, which well correspond to the different magnetic phases. We have proposed that the transport properties are consistently understood in terms of the spin-carrier phase separation below  $T_N$ .

The neutron powder diffraction using the high efficiency and high resolution measurements [11] were performed under the inter-university cooperative research program of the Institute for Materials Research, Tohoku University. This work was partially supported by MEXT, the Grant-in-Aid for Scientific Research (C), 2001, no.13640374.

---

\* Electronic address: sokat@htsc.sci.waseda.ac.jp

- [1] W. J. Zhu, P. H. Hor, A. J. Jacobson, G. Crisci, T. A. Albright, S. -H. Wang, and T. Vogt, *J. Am. Chem. Soc.* **119**, 12398 (1997).
- [2] M. Matoba, S. Okada, S. Fukumoto, S. Soyano, and H. Kitô, *Jpn. J. Appl. Phys.* **39 Suppl.**, 498 (2000).
- [3] S. Okada, M. Matoba, S. Fukumoto, S. Soyano, Y. Kamihara, T. Takeuchi, H. Yoshida, K. Ohoyama, and Y. Yamaguchi, *J. Appl. Phys.* **91**, 8861 (2002).
- [4] S. Okada, M. Matoba, H. Yoshida, K. Ohoyama, and Y. Yamaguchi, *J. Phys. Chem. Solids* **63**, 983 (2002).
- [5] C. Y. Chen, R. J. Birgeneau, M. A. Kastner, N. W. Preyer and T. Thio, *Phys. Rev.* **B 43**, 392 (1991).
- [6] J. B. Mandal, A. N. Das A N and B. Ghosh B, *J. Phys.: Condens. Matter* **8** 3047 (1996).
- [7] P. Lunkenheimer, V. Bobnar, A. V. Pronin, A. I. Ritus, A. A. Volkov, and A. Loidl *Phys. Rev.* **B 66**, 051105 (2002).
- [8] L. He, J. B. Neaton, M. H. Cohen, D. Vanderbilt, and C. C. Homes, *Phys. Rev.* **B 65**, 214112 (2002).
- [9] A. B. Pakhomov, S. K. Wong, X. Yan, and X. X. Zhang, *Phys. Rev.* **B 58**, R13375 (1998).
- [10] R. B. Laibowitz and Y. Gefen, *Phys. Rev. Lett.* **53**, 380 (1984).
- [11] K. Ohoyama, T. Kanouchi, K. Nemoto, M. Ohashi, T. Kajitani, Y. Yamaguchi, *Jpn. J. Appl. Phys.* **37**, 3319 (1998).